Differential dynamics and activity-dependent regulation of α- and β-neurexins at developing GABAergic synapses

Yu Fu[a,b] and Z. Josh Huang[a,1]

[a]Cold Spring Harbor Laboratory, Cold Spring Harbor, NY 11724; and [b]Program in Neuroscience, State University of New York, Stony Brook, NY 11790

Edited* by Thomas C. Südhof, Stanford University School of Medicine, Palo Alto, CA, and approved November 22, 2010 (received for review August 2, 2010)

Neurexins (NRXs) and neuroligins are key synaptic adhesion molecules that also recruit synaptic signaling machineries. Neurexins consist of α- and β-isoforms, but how they couple synaptic transmission and adhesion to regulate activity-dependent synapse development remains unclear, in part because of poor understanding of their cell biology and regulation in the relevant neurons. Here, we examined the subaxonal localization, dynamics, and regulation of NRX1α and NRX1β in cortical perisomatic inhibitory synapses. Both isoforms are delivered to presynaptic terminals but show significant and different turnover rate at the membrane. Although NRX1α is highly diffuse along developing axons and filopodia, NRX1β is strictly anchored at terminals through binding to postsynaptic ligands. The turnover rate of NRX1β is attenuated by neural activity and presynaptic $GABA_B$ receptors. NRXs, thus, are intrinsically dynamic but are stabilized by local transmitter release. Such an activity-adjusted adhesion system seems ideally suited to rapidly explore and validate synaptic partners guided by synaptic transmission.

surface dynamics | cell adhesion molecules

Synapse formation is a crucial component of neural circuit assembly. In the developing vertebrate CNS, synapse formation involves multiple steps (1–3). The initial contact of an axon with a potential postsynaptic target often leads to rapid initiation of transient synapse formation (4), which triggers the accumulation of adhesion molecules and recruitment of pre- and postsynaptic signaling machinery (1). These nascent synapses undergo an extensive process of validation (e.g., the matching of synapse types and transmitter and receptor types) and competition (for limited pre- and postsynaptic resources); only a subset of nascent contacts mature into more stable and functional synapses. A key mechanism for synapse validation and competition is the strength of synaptic transmission itself, but how synaptic activity regulates synaptic adhesion remains poorly understood. In particular, whether and how GABAergic transmission regulates synaptic adhesion at developing inhibitory synapses are largely unknown.

Neurexins (NRXs) and neuroligins (NLs) are arguably the best characterized synaptic adhesion molecules and have been implicated in the synapse formation process (5–7). Recent studies suggest that NLs contribute to activity-dependent specification and validation of synapses, with NL1 and NL2 acting on excitatory and inhibitory synapses, respectively (8). Because NRXs and NLs also bind and recruit pre- and postsynaptic signaling molecules, they seem ideally suited to couple synaptic signaling and adhesion. Current evidence implicates NRXs as a key mechanism that nucleates transsynaptic signaling, but whether and how neural activity regulates NRX property and function are unknown.

Vertebrate NRXs are encoded by three genes with extensive alternative splicing (9). Each gene contains two promoters that direct the synthesis of the longer α-NRX and shorter β-NRX, which share identical cytoplasmic tail but differ substantially in extracellular domains (10). It has been suggested that α- and β-NRX are not functionally redundant (11), but the significance of these isoforms remains unclear; whether they have distinct cell biological properties and are differentially regulated are unknown. Although NRXs and NLs are broadly expressed in the brain at both excitatory and inhibitory synapses, genetic studies in mice have revealed a particularly important role of both NRXs and NLs in the development and function of inhibitory synapses (11, 12). For example, knockin mice harboring the human autistic mutation R451C in NL3 show enhanced inhibitory transmission and impaired social interaction (13). Moreover, GABAergic transmission from Parvalbumin (PV)-positive neocortical interneurons, which form inhibitory synapses onto the soma and proximal dendrite of pyramidal neurons (i.e., perisomatic synapses), is selectively attenuated in NL2-deficient mice (14). These results suggest that subsets of inhibitory synapses and circuits are more vulnerable to perturbation of NRX–NL signaling and might contribute to pathogenic mechanisms of human mutations associated with neurodevelopmental disorders such as autism. It is, therefore, crucial to examine NRXs with cell- and synapse-type resolution in experimental systems that preserve basic neural circuit architecture.

We have established an experimental system that allows us to examine the localization, dynamics, and regulation of NRX isoforms with subcellular resolution in perisomatic inhibitory synapses of the mouse neocortex. We found that NRX1α and NRX1β are dynamically regulated by distinct mechanisms in developing GABAergic axons, which lead to profound differences in their subaxonal localization, trafficking, and activity-dependent regulation at presynaptic terminals. These different properties of α- and β-NRXs suggest distinct roles in activity-dependent synapse development.

Results

There are several major technical difficulties in studying the α- and β-NRX isoforms. First, the extensive sequence homology between these isoforms has precluded the generation of specific antibodies to distinguish them. Second, both isoforms are broadly expressed but may display cell or synapse type–specific properties, but there has been no strategy to visualize these isoforms in identified cell and synapse types with high resolution. Third, the membrane-inserted and intracellular pool of NRXs may have different localization and properties, but there has been no attempt to selectively visualize the membrane-inserted form that mediates transsynaptic signaling. Fourth, although it has been suggested that NRX–NL might mediate activity-dependent synapse formation, there has been no method to address whether NRXs are dynamically regulated by activity. We have developed methods and an experimental system to overcome these technical difficulties. To selectively visualize the membrane form of NRXs, we engineered a pH-sensitive pHluorin (SEP) in the extracellular domain of NRX1α (1α-SEP) and NRX1β (1β-SEP) (Fig. 1*A*). To visualize NRXs in a defined GABAergic neuron and synapse type, we developed a method to specifically

Author contributions: Y.F. and Z.J.H. designed research; Y.F. performed research; Y.F. analyzed data; and Y.F. and Z.J.H. wrote the paper.

The authors declare no conflict of interest.

*This Direct Submission article had a prearranged editor.

[1]To whom correspondence should be addressed. E-mail: huangj@cshl.edu.

This article contains supporting information online at www.pnas.org/lookup/suppl/doi:10.1073/pnas.1011233108/-/DCSupplemental.

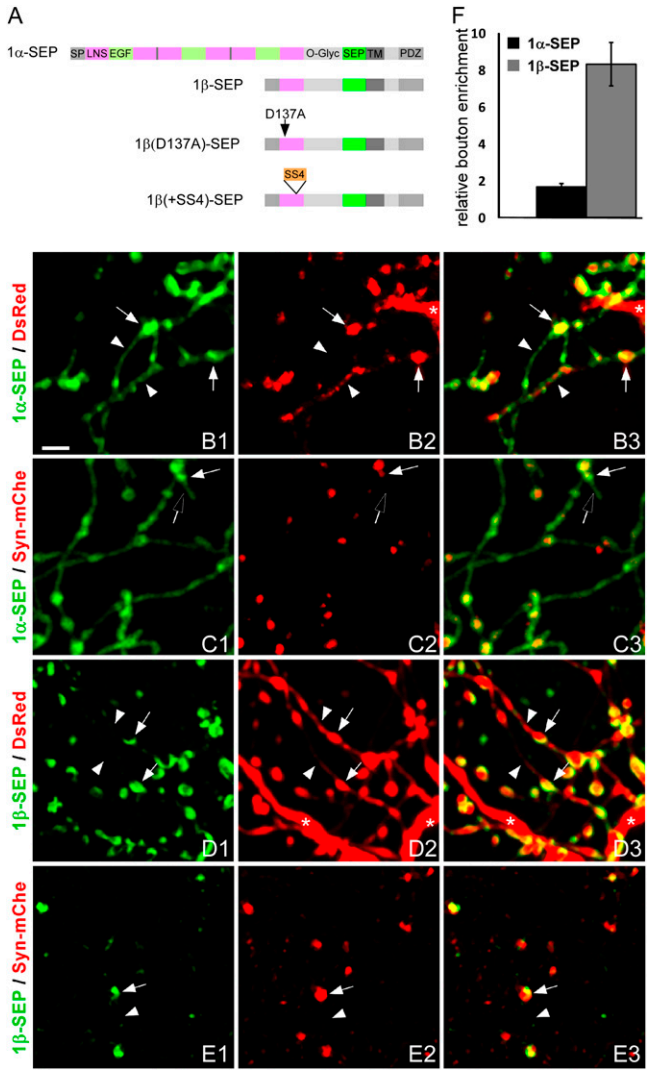

Fig. 1. Differential subcellular distribution of NRX1α and NRX1β in cortical PV basket interneurons. (*A*) SEP was inserted in the extracellular domain of the NRX1α, NRX1β, NRX1β(D137A), and NRX1β(+SS4) immediately after the transmembrane (TM) domain. All these NRX1 constructs share identical intracellular domains. Sparse PV neurons in cortical organotypic cultures from Pv-ires-Cre knockin mice were biolistically transfected at ~EP15 to coexpress NRX1-SEP and DsRed or synaptophysin-mCherry (Syn-mChe) using conditional expression vectors Lox-STOP-Lox(LSL)-NRX1-SEP, LSL-DsRed, and LSL-Syn-mChe. Live two-photon imaging was carried out at EP18 to EP20 (Fig. S1). (*B*) NRX1α-SEP signals were diffuse along the axon shaft (arrowheads) with some enrichment at boutons (arrows). (*C*) NRX1α-SEP signals readily spread to filopodia (open arrow), which extend from presynaptic boutons (labeled by Syn-mChe; white arrow in *C2*). Images were taken at 990 nm. (*D*) NRX1β-SEP signals were highly punctuate and restricted to subregions within presynaptic boutons (arrows). Note that boutons of similar size labeled by DsRed contained very different levels of NRX1β-SEP. (*E*) NRX1β-SEP signals highly colocalize with Syn-mChe. Arrowheads indicate axon shafts; asterisks indicate dendrites. (*F*) The relative enrichment of SEP signal on bouton vs. axon shaft was analyzed by quantifying the average SEP signal on bouton areas and the immediate nearby axon shaft; 10–15 boutons and nearby axon shafts from three to five neurons for each group were analyzed. (Scale bar: 2 μm.)

express the SEP-tagged NRXs in PV interneurons in organotypic cultures of mouse neocortex (Fig. S1). Using two-photon live cell imaging, we were able to examine the localization, dynamics, and regulation of NRX isoforms during the development of inhibitory synapses formed by PV interneurons.

Differential Subcellular Localization of NRX1α and NRX1β Along GABAergic Axons. The development of cortical perisomatic synapses and innervation pattern proceeds in organotypic cultures and is regulated by neural activity and GABA signaling (15, 16). We expressed 1α-SEP and 1β-SEP in PV interneurons from equivalent postnatal (EP) day 15 (Fig. S1*B*) when they are still actively extending axon branches and forming inhibitory synapse. We examined NRX1-SEP localization in axons at EP18 to EP20. We found that 1α-SEP was localized quite diffusely throughout the axon, including motile filopodia, with slight enrichment in presynaptic boutons (Fig. 1 *B* and *C*). In striking contrast, 1β-SEP was exclusively restricted to presynaptic terminals (Fig. 1 *D* and *E*). It is possible that the diffusive pattern of NRX1α is because of overexpression of NRX1α-SEP. If that was the case, we would expect to see lower relative bouton enrichment of NRX1α-SEP in cells expressing higher levels of NRX1α-SEP and higher relative bouton enrichment of NRX1α-SEP in cells expressing lower levels of NRX1α-SEP. We examined ~50 boutons and adjacent axon shafts from six different cells, which showed as much as sixfold difference in NRX1α-SEP levels (Fig. S2). There was either a slightly positive correlation or no correlation between the brightness of NRX1α-SEP and relative enrichment level on boutons; this indicated that higher expression of NRX1α-SEP did not lead to more diffusive distribution along axon.

We also examined if SEP tagging disrupted the binding with NL and thus, lead to artificial localization. Using HEK293T cells, we did not find significant difference between SEP-tagged NRXs and HA-tagged NRXs in binding with NL2 (Fig. S3). We then examined the subcellular localization of HA-NRX1α and HA-NRX1β in PV neurons by immunostaining surface-expressed HA under nonpermeabilized condition. We found that HA-tagged NRX1α and HA-NRX1β showed similar subcellular patterns as that in live neurons observed with SEP tagging (Fig. S4). These results provide compelling evidence for differential subaxonal localization of NRX1α and NRX1β, which must result from their different extracellular domains and interactions. Interestingly, presynaptic boutons of similar size often contained different amounts of 1β-SEP, which were further clustered to subregions within boutons (Fig. 1*D*, arrows). This raises the intriguing possibility that 1β-SEP might be restricted to the site of synaptic contact through binding to postsynaptic ligands.

Presynaptic Localization of NRX1β Is Dependent on Binding to Postsynaptic Ligands. We examined the role of postsynaptic NRX-binding ligands on the presynaptic clustering of 1β-SEP by taking advantage of the fact that NRX-NL binding is calcium-dependent. We first examined the effect of Ca^{2+} depletion on 1β-SEP localization by imaging before and after perfusing in EGTA-containing Ca^{2+}-free artificial cerebrospinal fluid (ACSF). EGTA treatment, which chelates extracellular Ca^{2+}, resulted in a rapid redistribution of 1β-SEP signals (the signal on bouton decreased 50.9% ± 5%, and the signal on the axon shaft increased 158.3% ± 30%); 1β-SEP signals became diffuse along axons, boutons, and filopodia within 5 min, leading to a significant decrease of the relative bouton enrichment of NRX-SEP signal (Fig. 2 *A*, *B*, and *E*). This result suggested that the presynaptic localization of 1β-SEP was Ca^{2+}-dependent and among other possibilities, might involve binding to NLs. We, thus, further examined the effects of an NRX1β mutant and splice variant, which show different binding affinity to NLs, on the localization of 1β-SEP. The crystal structure of the NRX–NL complex has been determined, and the calcium-binding pocket in NRX1 is located near its NL binding surface (17, 18). A single point mutation in NRX1, D137A, completely abolishes Ca^{2+} binding as well as NL binding (19); the same mutation also eliminates the ability of NRX1β to induce postsynaptic differentiation in dissociated neuron cultures (20). Here, we found that the D137A mutation, when introduced into 1β-SEP, resulted in diffuse localization of 1β(D137A)-SEP along the axon, a pattern resembling that of 1α-SEP (Fig. 2*C*). The clustering of 1β-SEP within boutons was also absent in the D137A mutant (Fig. 2*C*). We further examined a natural splicing variant of 1β with reduced affinity to NL. The splice site 4 containing (+SS4) NRX1β shows slightly but signifi-

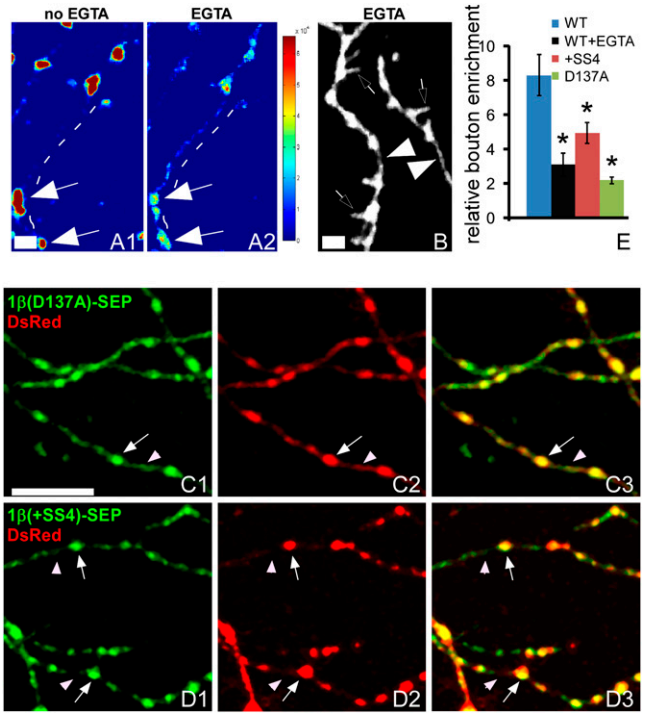

Fig. 2. The presynaptic localization of NRX1β-SEP depends on Ca^{2+} binding and postsynaptic ligands. (*A*) A PV neuron was labeled with Nrx1β-SEP and DsRed and imaged at EP20. SEP signals along axon segments are shown as heat maps under control condition (*A1*) or after 5 min of 5 mM EGTA treatment (*A2*) with the same gain and look-up table. Warmer colors represent higher fluorescent levels. Arrows indicate the presynaptic boutons; dotted lines delineate the axon shaft. (*B*) Immediate diffusion of NRX1β-SEP signals into the axon shaft (arrowhead) and filopodia (open arrow) within 5 min of EGTA treatment. (Scale bar: *A* and *B*, 2 μm.) (*C*) PV neurons were labeled with NRX1β(D137A)-SEP and DsRed. The D137A mutation, which abolishes binding to Ca^{2+} and NL, resulted in diffuse distribution of NRX1β (D137A)-SEP along axons. (*D*) PV cells were labeled with NRX1β(+SS4)-SEP and DsRed. This splice site 4-containing (+SS4) NRX1β variant with decreased binding affinity with NL2 showed significant presynaptic localization but was more diffusive along the axon shaft compared with NRX1β–SEP (Fig. 1). (Scale bar: *C* and *D*, 10 μm.) Arrows indicate boutons, and arrowheads indicate the axon shaft. (*E*) Quantification of the relative enrichment of SEP signals on bouton vs. adjacent axon shaft for WT 1β-SEP, β(D137A)-SEP, and 1β(+SS4)-SEP; 10–15 boutons and nearby axon shafts from three to five neurons for each group were analyzed. *$P < 0.05$ compared with WT value.

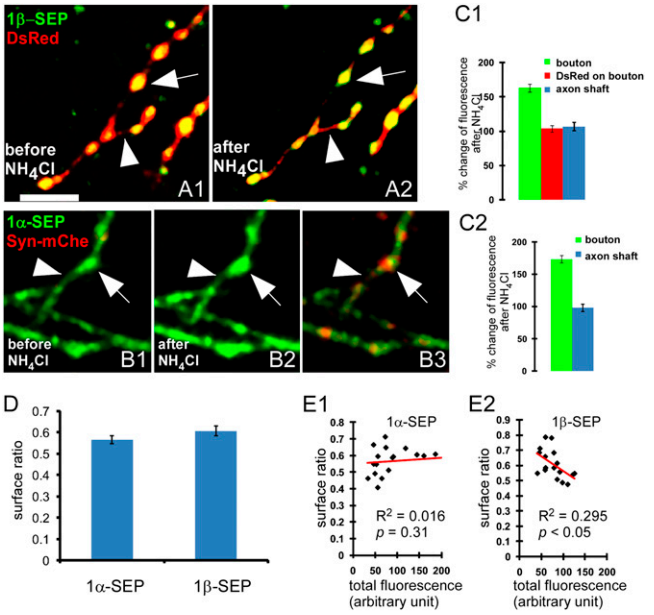

Fig. 3. Both NRX1α and NRX1β are mainly delivered to the axon membrane at presynaptic boutons. PV neurons expressing either NRX1β-SEP (*A*) or NRX1α-SEP (*B*) were imaged before and after NH_4Cl-containing ACSF to reveal the intracellular pool of SEP fusion proteins. NRX1α-SEP transfected neurons (*B3*) were also imaged at 990 nm to reveal presynaptic boutons labeled by Syn-mChe. Arrowheads indicate the axon shaft, and arrows indicate boutons. (Scale bar: *A* and *B*, 5 μm.) (*C*) The changes in SEP signal on boutons and axon shafts on NH_4Cl treatment were quantified for 1β-SEP (*C1*; $n = 18$ from three independent experiments) and 1α-SEP (*C2*; $n = 19$ from three independent experiments). (*D*) The changes in SEP signals were used to calculate the membrane fraction of 1α-SEP or 1β-SEP as a percentage of their total pool (method described in *SI Materials and Methods*). (*E*) The surface ratios of 1α-SEP and 1β-SEP were plotted against their total SEP signals from randomly selected boutons. The expression levels of 1α-SEP and 1β-SEP were comparable (horizontal axis in *E1* and *E2*). Although the surface ratio of 1α-SEP was independent of total 1α-SEP (*E1*), the surface fraction of 1β-SEP decreased with an increasing level of total 1β-SEP (*E2*).

cantly decreased binding affinity with NL2, which specifically localizes to GABAergic synapses (8, 20). 1β(+SS4)-SEP showed significant presynaptic localization (Fig. 2*D*, arrows) but was more diffusive along the axon shaft compared with 1β-SEP (Fig. 2*D*, arrowheads). The bouton enrichment level of 1β(+SS4)-SEP lay between those of the WT and D137A mutant (Fig. 2*E*). On being treated with EGTA, the 1β(+SS4)-SEP showed similar change as that of NRX1β-SEP, whereas 1β(D137A)-SEP showed no significant change on bouton and axon shaft (Fig. S5). Together, these results strongly suggest that NRX1β is anchored at presynaptic boutons through binding to postsynaptic ligand(s), likely NL2, and the binding affinity quantitatively influences its presynaptic and axonal localization pattern.

Both NRX1α and NRX1β Are Delivered to Presynaptic Terminals. The differential localization of 1α-SEP and 1β-SEP along PV cell axons raised the question of whether these two isoforms were delivered to the membrane from distinct intracellular compartments. We, thus, examined the total intracellular pool of 1α- and 1β-SEP. On NH_4Cl treatment, which neutralizes the pH of intracellular vesicles (21), the fluorescence signals of both 1α-SEP and 1β-SEP increased by ~60% at presynaptic terminals (Fig. 3 *A*–*C*). We determined that the portion of the membrane-inserted form of both 1α-SEP and 1β-SEP represented ~55% of their total pool (i.e., surface ratio) (Fig. 3*D* and *SI Materials and Methods*). Importantly, the increase in fluorescence signals for both 1α-SEP and 1β-SEP on NH_4Cl treatment was restricted in boutons but not along axon shafts (Fig. 3 *A* and *B*), indicating that the intracellular pools for both isoforms are localized to presynaptic terminals. The surface ratio for 1α-SEP was rather constant among terminals with significantly different levels of total pool; thus, more intracellular 1α-SEP likely leads to proportionally more membrane insertion. However, the surface ratio for 1β-SEP decreased with increasing levels of the total pool (Fig. 3*E*); thus, excessive supply of 1β-SEP does not proportionally increase the membrane-inserted 1β-SEP, suggesting more stringent regulation of 1β-SEP at the membrane independent of intracellular pool. Our results suggest that the intracellular pools of both NRX1α and NRX1β are transported to mature or nascent presynaptic terminals, where they are delivered to the membrane. Although 1α readily diffuses into axon shaft and filopodia and is only slightly enriched at the bouton membrane because of weak binding to putative postsynaptic ligands, 1β is strictly retained at the bouton because of its strong affinity to postsynaptic ligands.

Differential Dynamics of NRX1α and NRX1β at Presynaptic Boutons. Our SEP tagging of the extracellular domain of NRX1 further allowed us to examine the dynamic properties using fluorescence recovery after photo bleaching (FRAP). We found that both NRX1α and NRX1β were highly dynamic at presynaptic termi-

nals. 1β-SEP signals typically clustered to one side of the bouton membrane (Fig. 4*A*). After photo bleaching, 1β-SEP signals gradually recovered within 30 min but strictly at the same cluster within the bouton as before bleaching. Furthermore, the recovery process of 1β-SEP is significantly slowed down by inhibiting either clathrin-dependent endocytosis [25 μM myristalated dynamin peptide (myr-Dyn) for 30 min] or tetanus toxin-sensitive exocytosis [20 nM tetanus toxin (TeTx) for 1 h] (Fig. S6). This result indicated that NRX1β not only undergoes continuous and significant exo- and endocytosis but also is trafficked precisely to and from putative presynaptic contact sites. On the other hand, the diffuse axonal localization and fast recovery rate of NRX1α implied a role of passive diffusion in its membrane dynamics (Fig. 4*B*). Indeed, FRAP experiments on segments of axons with three successive boutons revealed that 1α-SEP signals in the middle bouton always recovered more slowly than those in the outer two, which were closer to unbleached pool and recovered with a similar rate (Fig. 4*C*). In addition, the recovery rate of 1α-SEP signals was independent of their axonal location (i.e., boutons and axon shaft), except proximity to unbleached diffusion pool (Fig. 4*D*). Together, our results suggest that NRX1β is continuously delivered and internalized at presynaptic boutons and is confined to presynaptic contact sites, likely through binding to postsynaptic ligands. However, the membrane-inserted NRX1α is more freely diffusible and engages in rapid exchange among neighboring pools along the axon shaft, presynaptic boutons, and filopodia. We speculate that the exo- and endocytosis of 1α-SEP at presynaptic terminals are similar to that of 1β-SEP, given their identical intracellular domain and intracellular pool, but the rapid diffusion of 1α-SEP in the membrane precluded a direct and precise examination of this property.

Activity-Dependent Regulation of Presynaptic NRX1β Dynamics. Because NRXs and NLs have been implicated in activity-dependent synapse development, we examined whether the dynamics (or stability) of NRX1 were regulated by neural activity. PV interneurons show significant spontaneous firing in cortical organotypic cultures. We found that acute blockade of sodium channel-dependent spiking activity by tetrodotoxin (TTX) resulted in a significant increase in the recovery rate of 1β-SEP after photo bleaching. This effect of TTX was mimicked by a $GABA_BR$ antagonist, CGP46381 (CGP), and reversed by a $GABA_BR$ agonist (baclofen) (Fig. 5*A*). However, this acute treatment of TTX and CGP did not result in significant change of the surface ratio of 1β-SEP (Fig. S7), suggesting that the trafficking machinery and surface stability of Nrx1β but not the total surface population of Nrx1β are more sensitive to the acute blockade of activity and GABA signaling. These results suggest that activity increases the stability (or suppresses the dynamics) of the membrane-inserted form of 1β-SEP at presynaptic terminals in part through GABA release and $GABA_BR$ signaling. Because $GABA_BRs$ localize to axon terminals of PV cells as well as to other postsynaptic sites, we used a single cell genetic strategy to examine the cell autonomous role of $GABA_BR$ in regulating the dynamics of 1β-SEP in PV axons (Fig. S1*A3*). Deletion of the *$GABA_{B1}$* gene in a single PV neuron resulted in increased dynamics of 1β-SEP at presynaptic terminals and also rendered the dynamics insensitive to the $GABA_BR$ antagonist (Fig. 5*B*). These results suggest that presynaptic $GABA_BR$ signaling in PV cells locally regulates trafficking and stability of membrane-inserted NRX1β. However, the dynamics of 1α-SEP were not affected by either TTX or CGP (Fig. 5*C*). It is possible that the exo- and endocytosis of 1α-SEP at presynaptic boutons might also be regulated by neural activity and $GABA_BR$ signaling, but this could not be detected by our FRAP assay because of the free diffusion of 1α-SEP along axon membrane.

Discussion

Recent studies expand the ligands of NRXs from NLs to leucine-rich repeat transmembrane protein 2, a member of another family of postsynaptic adhesion molecules implicated in synapse development (22, 23). NRXs, therefore, represent a key presynaptic mechanism that nucleates transsynaptic signaling. A prominent feature of NRXs is the presence of α- and β-isoforms, and one of their most appealing properties is the potential to directly couple synaptic transmission and adhesion. Although studies using artificial synapse formation assays and dissociated neuronal cultures have provided major insights into several basic properties of NRXs, whether and how α- and β-NRXs mediate activity-dependent synapse formation and validation remain largely un-

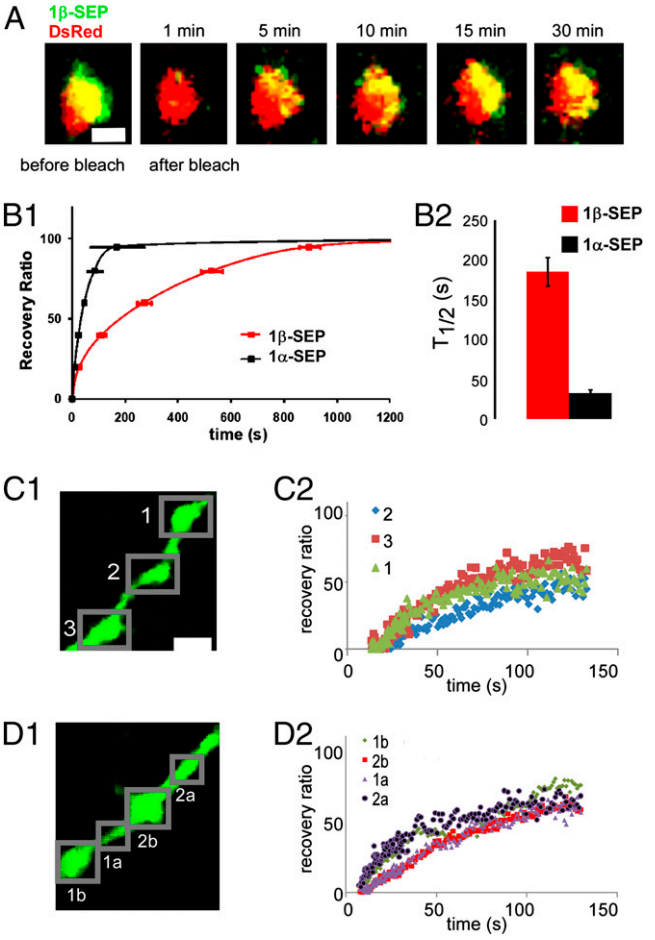

Fig. 4. Dynamic turnover of NRX1α and NRX1β at presynaptic terminals through distinct mechanisms. Presynaptic boutons with a diameter of 1–1.5 μm and located more than 15 μm from branch points were chosen for FRAP. (*A*) Representative FRAP of NRX1β-SEP on a single bouton. Recovery after photo bleaching was imaged at 1-s intervals during the first 100 s and then at 20-s intervals for another 30 min. Note that 1β-SEP signals clustered to one side of the bouton before bleaching and recovered ~30 min after bleaching to precisely the same cluster. (Scale bar: 1 μm.) (*B1*) Averaged recovery curves for 1α-SEP (eight boutons from eight cells in three independent experiments) and 1β-SEP (10 boutons from 10 cells in three independent experiments). The recovery ratio was normalized to the plateau fluorescence after 1,000 s of recovery. (*B2*) $T_{1/2}$ (the time to reach one-half of the plateau level) was determined with curve fitting as described in *SI Materials and Methods*. Note that 1α-SEP recovered approximately six times faster than 1β-SEP. (*C* and *D*) The fast recovery of 1α-SEP after photo bleaching results from free diffusion along the axon membrane. (*C1*) Representative two-photon image and FRAP of 1α-SEP on an axon segment with three boutons (boxed as 1, 2, and 3). (*C2*) The 1α-SEP signal in the middle bouton 2 always recovered more slowly than those in the outer two (1 and 2), which were closer to the unbleached pool and recovered with a similar rate. (*D1*) FRAP of 1α-SEP on an axon segment with two boutons (1b and 2b) and two areas of axon shafts (1a and 2a). The recovery rate of the 1α-SEP signal was independent of the axonal location (i.e., boutons vs. axon shaft), except for proximity to the unbleached diffusion pool (*D2*). (Scale bar: *C1* and *D1*, 2 μm.)

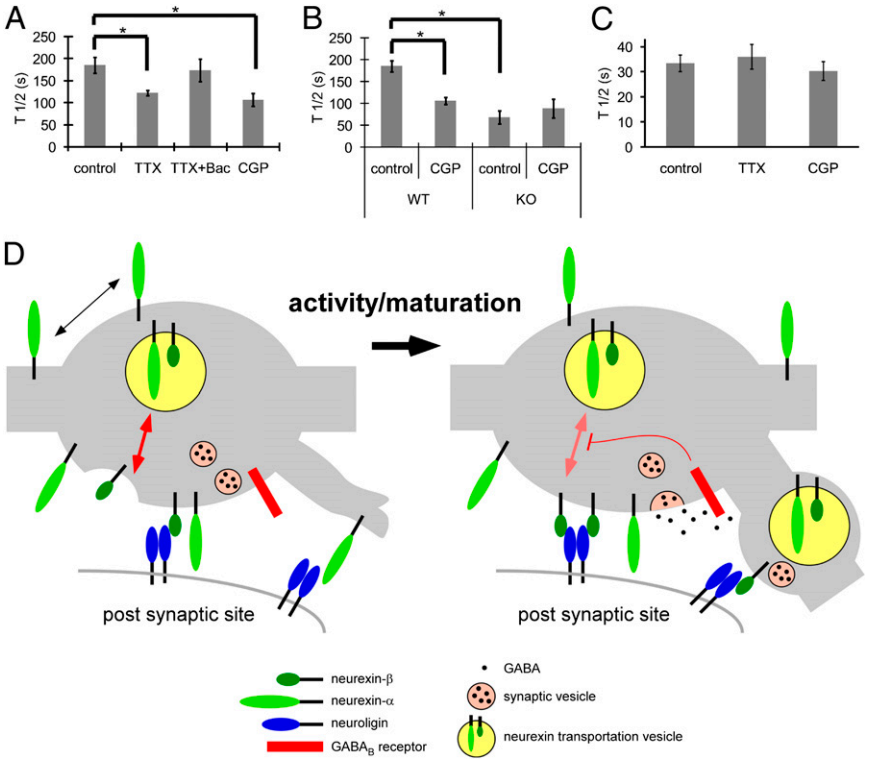

Fig. 5. Activity-dependent regulation of NRX1β turnover at presynaptic boutons. (*A*) PV neurons expressing NRX1β-SEP and DsRed in EP21 slice cultures were treated with 1 μM TTX, 1 μM TTX and 10 μM baclofen (Bac), or 10 μM CGP46328 (CGP) for 30 min before FRAP experiments. The turnover rate of 1β-SEP was measured as $T_{1/2}$ (8–10 boutons from 8 to 10 cells in three independent experiments for each condition). TTX treatment increased the turnover rate; this effect was mimicked by CGP46328 and rescued by Bac. (*B*) Presynaptic GABA$_B$Rs in PV neurons regulate NRX1β dynamics at boutons. Cortical slice cultures from *GABA$_{B1}^{flx/flx}$* mice were transfected with P_{Gad1}-Nrx1β-SEP and P_{Gad1}-TdTomato, with (KO) or without (WT) P_{Gad1}-Cre (Fig. S1*A3*). Compared with WT PV neurons (WT), *GABA$_B$*R-deficient PV neurons (KO) showed increased turnover rate of 1β-SEP at presynaptic boutons and were no longer sensitive to CGP46328 (*$P < 0.05$; five boutons from five cells in three independent experiments for each group). (*C*) The turnover rate of NRX1α-SEP at PV axon terminals was not influenced by neural activity. PV neurons expressing NRX1α-SEP and Syn-mCherry were treated with 1 μM TTX or 10 μM CGP for 30 min before FRAP experiment. (*D*) A model on the distinct role of NRX1α and NRX1β in activity-dependent development of GABAergic synapses. Both NRX1α and NRX1β are transported to nascent or mature presynaptic boutons and are dynamically delivered to and internalized from the presynaptic membrane. The rapid and free diffusion of NRX1α to the axon and filopodia may serve as an exploring mechanism to search for potential postsynaptic partners throughout the axon path. A potential postsynaptic site (e.g., an NL2 cluster) can initiate weak binding to NRX1α and in turn, recruit presynaptic GABA release machinery. NRX1β is restricted to the presynaptic membrane by engaging in high-affinity binding to NL2 and is further stabilized by GABA release and presynaptic GABA$_B$R signaling, which reduces the turnover rate of NRX1β. A positive feedback between GABA release and NRX1β-NL2 binding could promote activity-dependent strengthening of nascent synaptic contact.

clear. This is in part because of our poor understanding of the cell biology of these isoforms and their regulation in relevant neurons and synapses within their native neural circuits. Here, we established a strategy to examine the membrane-inserted form of α- and β-NRXs at a defined class of cortical GABAergic synapses that is shown to be particularly sensitive to NL2 perturbation (14). We discovered that NRX1α and NRX1β in developing GABAergic axons are dynamically regulated by distinct mechanisms, which lead to profound differences in their subaxonal localization, dynamic turnover, and activity-dependent regulation at presynaptic terminals; these different properties suggest distinct roles for α-and β-NRXs in inhibitory synapse development and function.

Using pHluorin tagging to distinguish the membrane vs. intracellular pool, we found that the intracellular pools of both 1α and 1β are transported to presynaptic terminals, where they are delivered to the membrane. It is possible that the identical cytoplasmic domain of 1α and 1β engages the same intracellular trafficking machinery (24). Upon exocytosis, however, 1α and 1β show strikingly different properties, likely because of their different extracellular domains and interactions. Although 1α is highly diffuse along the axon shaft, boutons, and filopodia, 1β is strictly anchored at boutons or synaptic contact sites through binding to postsynaptic ligands. A particularly significant finding is the high turnover rate of 1α and 1β at presynaptic membrane. Synaptic adhesion molecules are generally thought of as molecular glues that join pre- and postsynaptic membranes and provide structural support and stability. On the other hand, dynamic regulation of adhesion molecules could serve as a key mechanism during synapse formation, specification, validation, and plasticity, especially when regulated by neural activity; however, evidence for dynamic trafficking of adhesion molecules is scarce (25). Our FRAP experiments revealed surprisingly high and yet different turnover rates for 1α and 1β at developing presynaptic terminals. Because NRX1β is largely confined to synaptic contact sites by binding to postsynaptic ligands, its turnover likely results from the continuous endo- and exocytosis at the presynaptic terminal. For NRX1α, however, both endocytosis at the terminal and diffusion along axon membrane may contribute to its more rapid dynamics. Such dynamic trafficking of NRXs provides a cell biological basis for regulation by neural activity. Indeed, we found that the dynamic and continuous turnover of membrane-inserted NRX1β seems to be an intrinsic property that is suppressed by neural activity. Importantly, we provide significant evidence that the activity-dependent decrease of NRX1β turnover, thus, stabilization, at presynaptic sites is mediated by GABA–GABA$_B$R signaling, which likely localizes at or near the same presynaptic terminal (26). Such a GABA$_B$R-mediated and potentially bouton autonomous regulation of NRX1β stability provides a plausible mechanism for a direct coupling of synaptic transmission and adhesion.

Our results suggest a model that implicates NRXs in activity-dependent synapse development (Fig. 5*D*). The rapid and free diffusion of NRX1α along the axon and filopodia combined with its large extracellular domain may serve as a widespread exploring mechanism to search for potential postsynaptic partners throughout the immediate vicinity of the axon arbor. A potential postsynaptic site (e.g., an NL2 cluster) can initiate weak binding to NRX1α and in turn, recruit presynaptic GABA release machinery through CASK (calcium/calmodulin-activated serine protein kinase) and associated proteins. Importantly, NRX1β is also dynamically delivered to developing presynaptic terminals, engages in high-affinity binding to NL2, and is further stabilized by presynaptic GABA release and GABA$_B$R signaling. The finding that presynaptic enrichment of NRX1β depends on ligand binding (Fig. 2) but punctuate NL distribution on postsynaptic membrane is independent of NRXs (27) suggests that preassembled NL2 clusters might trigger and then promote presynaptic differentiation. Therefore, a positive feedback between GABA release and NRX1β–NL2 binding could promote activity-dependent strengthening of developing synaptic contact. Our studies, therefore, suggest the concept that NRXs (and NLs) represent an intrinsically

dynamic synaptic adhesion system that is stabilized by appropriate synaptic activity. Such activity-dependent local adjustment of adhesion molecules seems ideally suited to rapidly explore potential synaptic partners, validate appropriate partners, and promote synapse formation guided by synaptic activity.

Our findings raise a number of questions regarding the mechanisms of NRX1 trafficking and regulation. The rapid exo- and endocytosis of NRX1 are likely carried out by vesicular transport and fusion machinery that are distinct from those of synaptic vesicles, but the identity, property, and regulation of this machinery are unclear, although the experiments with myr-Dyn and TeTx suggested that efficient membrane recycling is involved in NRX1 trafficking. In addition, the mechanism by which $GABA_BR$ regulates NRX1β remains to be defined. $GABA_BR$ is a $G_{i/o}$-coupled receptor (28). The $G_{i/o}$ signaling pathway has been implicated in regulating axon dynamics by promoting actin polymerization and inhibiting depolymerization or severing (29). Interestingly, actin filaments regulate synaptic vesicle trafficking at multiple steps (3) and are linked to NRXs through CASK, which nucleates the assembly of actin on the cytoplasmic domain of NRXs (30). It is, therefore, plausible that presynaptic $GABA_BRs$ might influence NRX1β trafficking and stability by regulating actin dynamics.

We have shown that GABA signaling and $GABA_B$ receptors in PV interneurons regulate activity-dependent development of perisomatic inhibitory synapses in postnatal neocortex (16). Our current finding suggests a possible mechanism by which NRX1β couples GABA-mediated synaptic signaling to synaptic adhesion and structural/functional modification. This hypothesis needs to be tested by perturbing the function and dynamic properties of NRX isoforms and examining the effects on synapse development. On the postsynaptic side, recent studies indicate that NL2 drives postsynaptic assembly of perisomatic inhibitory synapses through gephrin and collybistin, which recruit $GABA_A$ receptors (31). There is also evidence that $GABA_ARs$ contribute to synapse structure in addition to GABA transmission (32). Whether NL2 at the postsynaptic membrane is dynamically regulated by neural activity and $GABA_AR$ signaling and whether such regulations influence binding to presynaptic NRXs remain to be examined.

Materials and Methods

Mice. $GABA_{B1}{}^{flx/flx}$ mice are a gift from Dr. Bernhard Bettler (University of Basel, Basel, Switzerland). Pv-ires-Cre mice are a gift from Dr. Silvia Arber (University of Basel, Basel, Switzerland).

Constructs. Constructs were generated as described in detail in *SI Materials and Methods*.

Slice Culture and Biolistic Transfection. Slice culture was performed as described previously (15). Biolistic transfections were performed as described in detail in *SI Materials and Methods*.

Two-Photon Imaging. Living slice preparations were imaged using a custom-built two-photon laser scanning microscope based on a Fluoview laser scanning microscope (Olympus America). We used a 60× objective (NA 0.9; Olympus), and the light source was a Ti-Sapphire laser (Chameleon Ultra; Coherent) with tunable wavelength. Images were taken at 910 nm unless otherwise stated. The laser power was monitored by a custom-built power meter. Fluorescence was detected in whole-field detection mode with a photomultiplier tube (Hamamatsu). FRAP experiments and NH_4Cl experiments were performed as described in detail in *SI Materials and Methods* and Fig. S8.

Statistics. Results are shown as mean ± SEM; statistical differences between two groups of data were evaluated using a nonpaired student *t* test. All experiments were performed with at least three independent replicates. Differences were considered significant for $P < 0.05$.

ACKNOWLEDGMENTS. We thank Drs. Linda Van Alest and Gary Matthews for helpful comments on the manuscript. The work is supported by a grant from the Harold and Leila Mathers Foundation.

1. Waites CL, Craig AM, Garner CC (2005) Mechanisms of vertebrate synaptogenesis. *Annu Rev Neurosci* 28:251–274.
2. Niell CM, Smith SJ (2004) Live optical imaging of nervous system development. *Annu Rev Physiol* 66:771–798.
3. Dillon C, Goda Y (2005) The actin cytoskeleton: Integrating form and function at the synapse. *Annu Rev Neurosci* 28:25–55.
4. Chao DL, Ma L, Shen K (2009) Transient cell-cell interactions in neural circuit formation. *Nat Rev Neurosci* 10:262–271.
5. Südhof TC (2008) Neuroligins and neurexins link synaptic function to cognitive disease. *Nature* 455:903–911.
6. Scheiffele P, Fan J, Choih J, Fetter R, Serafini T (2000) Neuroligin expressed in nonneuronal cells triggers presynaptic development in contacting axons. *Cell* 101: 657–669.
7. Graf ER, Zhang X, Jin SX, Linhoff MW, Craig AM (2004) Neurexins induce differentiation of GABA and glutamate postsynaptic specializations via neuroligins. *Cell* 119:1013–1026.
8. Chubykin AA, et al. (2007) Activity-dependent validation of excitatory versus inhibitory synapses by neuroligin-1 versus neuroligin-2. *Neuron* 54:919–931.
9. Ullrich B, Ushkaryov YA, Südhof TC (1995) Cartography of neurexins: More than 1,000 isoforms generated by alternative splicing and expressed in distinct subsets of neurons. *Neuron* 14:497–507.
10. Tabuchi K, Südhof TC (2002) Structure and evolution of neurexin genes: Insight into the mechanism of alternative splicing. *Genomics* 79:849–859.
11. Missler M, et al. (2003) Alpha-neurexins couple Ca2+ channels to synaptic vesicle exocytosis. *Nature* 423:939–948.
12. Varoqueaux F, et al. (2006) Neuroligins determine synapse maturation and function. *Neuron* 51:741–754.
13. Tabuchi K, et al. (2007) A neuroligin-3 mutation implicated in autism increases inhibitory synaptic transmission in mice. *Science* 318:71–76.
14. Gibson JR, Huber KM, Südhof TC (2009) Neuroligin-2 deletion selectively decreases inhibitory synaptic transmission originating from fast-spiking but not from somatostatin-positive interneurons. *J Neurosci* 29:13883–13897.
15. Chattopadhyaya B, et al. (2004) Experience and activity-dependent maturation of perisomatic GABAergic innervation in primary visual cortex during a postnatal critical period. *J Neurosci* 24:9598–9611.
16. Chattopadhyaya B, et al. (2007) GAD67-mediated GABA synthesis and signaling regulate inhibitory synaptic innervation in the visual cortex. *Neuron* 54:889–903.
17. Araç D, et al. (2007) Structures of neuroligin-1 and the neuroligin-1/neurexin-1 beta complex reveal specific protein-protein and protein-Ca2+ interactions. *Neuron* 56: 992–1003.
18. Fabrichny IP, et al. (2007) Structural analysis of the synaptic protein neuroligin and its beta-neurexin complex: Determinants for folding and cell adhesion. *Neuron* 56: 979–991.
19. Reissner C, Klose M, Fairless R, Missler M (2008) Mutational analysis of the neurexin/neuroligin complex reveals essential and regulatory components. *Proc Natl Acad Sci USA* 105:15124–15129.
20. Graf ER, Kang Y, Hauner AM, Craig AM (2006) Structure function and splice site analysis of the synaptogenic activity of the neurexin-1 beta LNS domain. *J Neurosci* 26:4256–4265.
21. Sankaranarayanan S, De Angelis D, Rothman JE, Ryan TA (2000) The use of pHluorins for optical measurements of presynaptic activity. *Biophys J* 79:2199–2208.
22. Ko J, Fuccillo MV, Malenka RC, Südhof TC (2009) LRRTM2 functions as a neurexin ligand in promoting excitatory synapse formation. *Neuron* 64:791–798.
23. de Wit J, et al. (2009) LRRTM2 interacts with Neurexin1 and regulates excitatory synapse formation. *Neuron* 64:799–806.
24. Fairless R, et al. (2008) Polarized targeting of neurexins to synapses is regulated by their C-terminal sequences. *J Neurosci* 28:12969–12981.
25. Tai CY, Mysore SP, Chiu C, Schuman EM (2007) Activity-regulated N-cadherin endocytosis. *Neuron* 54:771–785.
26. Gonchar Y, Pang L, Malitschek B, Bettler B, Burkhalter A (2001) Subcellular localization of GABA(B) receptor subunits in rat visual cortex. *J Comp Neurol* 431: 182–197.
27. Dresbach T, Neeb A, Meyer G, Gundelfinger ED, Brose N (2004) Synaptic targeting of neuroligin is independent of neurexin and SAP90/PSD95 binding. *Mol Cell Neurosci* 27:227–235.
28. Bettler B, Kaupmann K, Mosbacher J, Gassmann M (2004) Molecular structure and physiological functions of GABA(B) receptors. *Physiol Rev* 84:835–867.
29. Luo L (2002) Actin cytoskeleton regulation in neuronal morphogenesis and structural plasticity. *Annu Rev Cell Dev Biol* 18:601–635.
30. Biederer T, Sudhof TC (2001) CASK and protein 4.1 support F-actin nucleation on neurexins. *J Biol Chem* 276:47869–47876.
31. Poulopoulos A, et al. (2009) Neuroligin 2 drives postsynaptic assembly at perisomatic inhibitory synapses through gephyrin and collybistin. *Neuron* 63:628–642.
32. Essrich C, Lorez M, Benson JA, Fritschy JM, Lüscher B (1998) Postsynaptic clustering of major GABAA receptor subtypes requires the gamma 2 subunit and gephyrin. *Nat Neurosci* 1:563–571.